Bioorganic & Medicinal Chemistry 20 (2012) 4012–4019

Contents lists available at SciVerse ScienceDirect

Bioorganic & Medicinal Chemistry

journal homepage: www.elsevier.com/locate/bmc

Effects of chemical modification of sphingomyelin ammonium group on formation of liquid-ordered phase

Sarah A. Goretta [a], Masanao Kinoshita [b], Shoko Mori [a], Hiroshi Tsuchikawa [a], Nobuaki Matsumori [a], Michio Murata [a,b,*]

[a] Department of Chemistry, Graduate School of Science, Osaka University, 1-1 Machikaneyama, Toyonaka, Osaka 560-0043, Japan
[b] JST ERATO, Lipid Active Structure Project, 1-1 Machikaneyama, Toyonaka, Osaka 560-0043, Japan

ARTICLE INFO

Article history:
Received 27 March 2012
Revised 8 May 2012
Accepted 8 May 2012
Available online 15 May 2012

Keywords:
Lipid raft
Sphingomyelin
Cholesterol
Lipid ordered phase

ABSTRACT

Sphingomyelin (SM) and cholesterol form microdomains called lipid rafts in cellular membranes. To develop a versatile fluorescent lipid probe, chemical modifications to both the hydrophobic and hydrophilic portions of SM are essential. Few reports describing SM probes with a fluorophore at the polar head group have been published. This study examined the effect of substitution on an ammonium moiety of SM on the membrane properties of SM. Two SM analogs with small propargyl and allyl groups on the quaternary nitrogen atom were synthesized and subjected to analysis using differential scanning calorimetry, fluorescent anisotropy, detergent solubilization, surface pressure, and density measurements. Results demonstrated that the two SM analogs retained the membrane properties of SM, including formation of an ordered phase and the ability to interact with cholesterol. A dansyl-substituted SM was prepared for fluorescent measurements. Dansyl-SM showed less of a propensity to form microdomains. These findings imply the potential application of N-substituted SMs as a raft-specific molecular probe.

1. Introduction

Lipid rafts are microdomains enriched in sphingomyelin (SM), cholesterol (Chol), and proteins, and form a liquid-ordered phase that is resistant to solubilization by Triton X-100.[1] These membrane domains play important roles in signal transduction,[2] and so membrane biophysical studies require them to be visualized either by using a fluorescent lipid probe or by fluorescent proteins that interact specifically with sphingomyelin-binding domains (SBD). However, current lipid probes that possess a fluorophore in the hydrophobic acyl portions can alter the distribution and dynamics of lipids,[3] hence making the observation of lipid rafts a challenge. Although a few fluorescent-labeled SMs in the polar head have been reported,[4] their membrane properties, particularly those of raft formation, have not been characterized.

Detection of intermolecular interactions between SMs and specific SBD-proteins could produce information essential for understanding the cellular functions of lipid rafts. Fluorescent resonance energy transfer (FRET) is a promising technique for detecting such interactions occurring in nanoscale domains. To observe the original protein–lipid interactions occurring on the surface of biomembranes through FRET experiments,[5] a relatively small fluorescence label needs to be introduced into the hydrophilic part of the lipid that is recognized by SBD proteins. In addition, an intrinsic fluorophore such as tryptophan is preferable for locating the residues responsible for lipid recognition.

This study describes the synthesis of SM analogs through modification of a trimethylammonium moiety, and characterizes their raft-forming properties for evaluating the possibility of developing a fluorescence-labeled SM probe of physiological relevance.

2. Results

2.1. Design and synthesis of SM probes

For conversion from L-serine to a protected sphingosine or its equivalents, a method reported by Blot et al.[6] (or partly by others[7]) was basically adapted with some modifications (Scheme 1). Briefly, the stereocontrolled condensation of 1-pentadecyne with Garner aldehyde **5** was followed by Birch reduction as the key steps, leading to the protected sphingosine **6**. Modification of the method by Sandbhor[4] provided a cyclic phospholane and subsequent ring opening with *N,N*-dimethyl-*N*-propargylamine yielded the protected lyso-SM 8 in a single step. A possible improvement in this step is formation of the head group under non-acidic conditions, which simplifies the scheme considerably by eliminating the need for several steps for the conversion to azide and regeneration of an amino group; previously,[4] they used a 2-azide derivative of **7** for phosphocholine substitution reaction probably due to treatment

* Corresponding author. Tel./fax: +81 66850 5774.
E-mail address: murata@chem.sci.osaka-u.ac.jp (M. Murata).

0968-0896/$ - see front matter © 2012 Elsevier Ltd. All rights reserved.
http://dx.doi.org/10.1016/j.bmc.2012.05.015

with TMSOTf. In the present Scheme 1, *N*-Boc intermediate **7** directly derived from *N*-Boc-Lys could be subjected the reaction. After removal of Boc and PMB protection groups, treatment with stearic nitrophenyl ester led to progargyl-SM 2; synthesis of **2** from sphingosine has been reported by the same authors.[4] Use of a dansyl fluorophore that has an excitation wavelength of 340 nm was motivated by the possibility to measure FRET with a tryptophan residue that emits fluorescence ca. 340 nm in SBD proteins such as lysenin. The azide functionality was introduced in the fluorophore for click chemistry with the propargyl group of **2** using the method of Kim et al. (Scheme 1).[8] The final click coupling proceeded smoothly to furnish dansyl-SM **4**. A similar click reaction using **2** has been reported for another fluorophore by Sandbhor et al.[4] An allyl group was chosen as another tether group because metathesis reactions, which usually involve terminal olefins specifically, can be used to introduce a labeling group. Use of allyldimethylamine facilitated the introduction of a modified choline moiety in step **e** of Scheme 1, as compared with its propargyl counterpart. The SM analogs **2**, **3**, and **4** were efficiently prepared and their membrane properties evaluated.

2.2. Measurement of phase transition temperature and order of membranes with analogs

Phase transition temperature T_m, a basic property of membrane lipids, was measured by differential scanning calorimetry (DSC) for stearoylSM (SSM) and analogs **2** and **3** as their hydrated bilayer preparations. The T_m values of **1**, **2**, and **3** were 42.5, 40.6, and 39.5 °C, respectively (DSC traces are provided as Supplementary data). Analogs **2** and **3** possessed T_m values similar to that of SSM **1**, implying that a small substituent on the ammonium moiety did not greatly alter the intermolecular interactions in a membrane form. We attempted to prepare bilayer vesicles from dansyl analogue **4**, but it was found that **4** fails to form stable bilayers in the absence of Chol. Thus, we carried out fluorescent anisotropy and specific volume experiments using the bilayer preparations of **1**, **2** and **3** (not **4**). Instead, we performed surface pressure measurements using the monolayers of **4** in comparison with those of **1**, **2** and **3**.

Fluorescent anisotropy experiments, done to evaluate the order of membrane lipids, were conducted with membrane preparations consisting of 100% SSM, **2** and **3** to determine the influence of ammonium functionality modification on membrane properties (Fig. 1). As with the T_m measurements, hydrated bilayers composed entirely of **2** and **3** showed an order similar to that of SMM, as indicated by temperature-dependent changes in the fluorescence anisotropy **r** of membrane-bound diphenylhexatriene. Slight shifts in the temperature for inflection points are due to the lower T_m values of **2** and **3** as compared with that of **1**.

2.3. Detergent solubilization of SSM analogs

Detergent solubilizing assays were conducted for SM analogs **2**, **3**, and **4** and compared to that of SSM, **1**. After treatment with 0.5% Triton-X, formation of lipid microdomains was evaluated by percentage of retained light scattering, measured as optical density at 400 nm. As shown in Figure 2, allyl- and propargyl-substituted analogs **2** and **3** gave rise to percentages similar to that of SSM in the presence of 50% cholesterol (Chol), which is supposed to form an SM raft-like ordered phase. Upon addition of 33% palmitoyl oleoyl phosphatidyl choline (POPC) and 33% Chol, SSM underwent phase separation, leading to formation of an SM/Chol-rich *Lo* phase and a POPC-rich *Ld* phase. Under these conditions, analogs **2** and **3** showed significant formation of insoluble domains as in the case with an SSM/Chol system (Fig. 2). In contrast, dansyl-substituted **4** produced a significantly lower amount of detergent-insoluble domains both in SM-Chol and SM-PC-Chol systems. However, as compared with POPC-Chol systems, which usually produce values of less than 5% scattering,[9] **4** retained some ability to form a lipid ordered phase.

2.4. Interactions between SM analogs and cholesterol

We examined intermolecular interaction of each SM analogue with Chol. First, the surface pressure versus molecular area (π–A) isotherms for pure SM, pure Chol and SM/Chol monolayers at 25.0 ± 0.1 °C are shown in Figure 3. The isotherm for the pure **1** monolayer showed a low slope region (π = 10–20 mN/m)

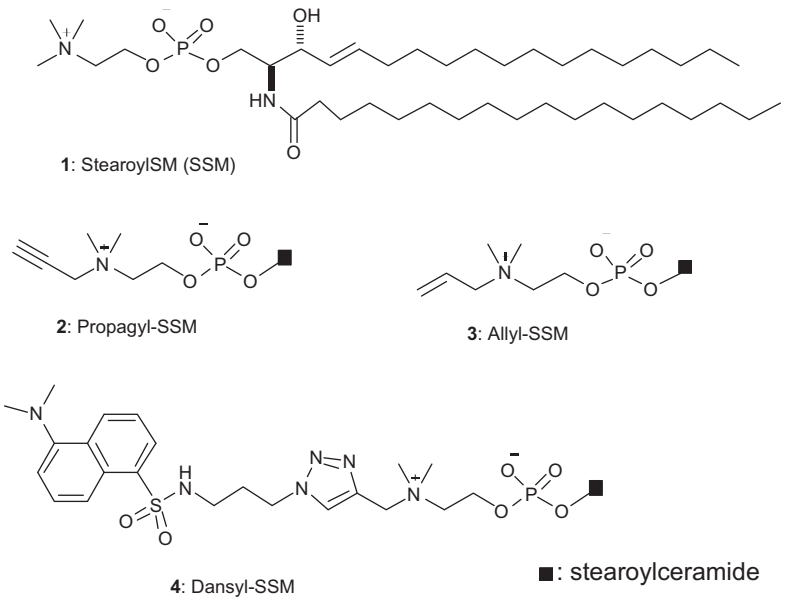

Structures. SSM **1** and analogs **2**, **3**, and **4**.

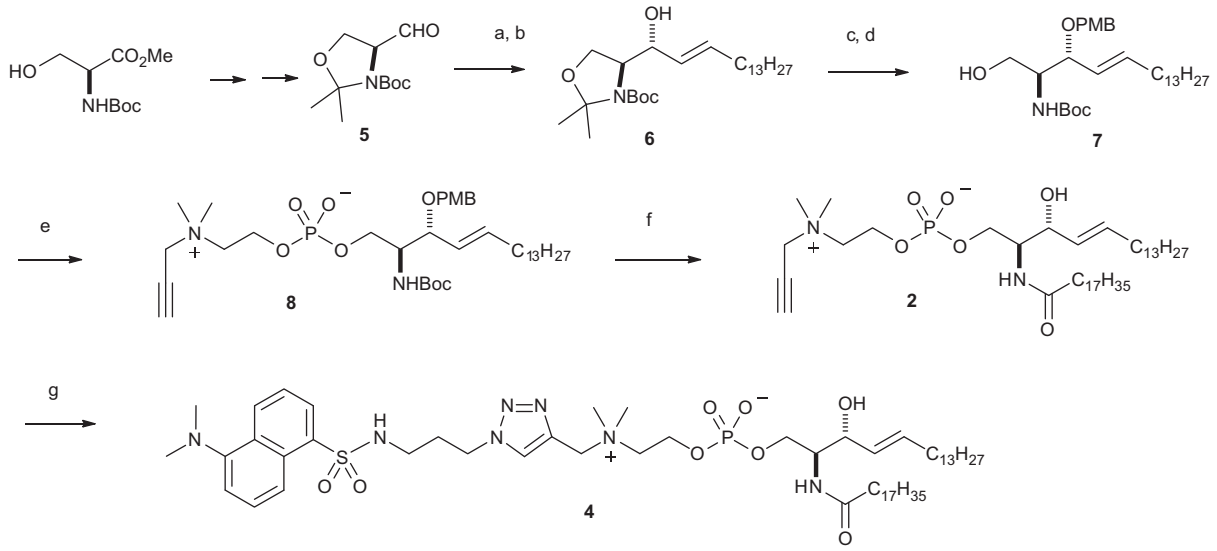

Scheme 1. Synthesis of propargyl SM **2** and dansyl SM **4** from Garner aldehyde. Reagents and conditions: (a) *n*-BuLi, 1-pentadecyne, THF, −20 °C, 3 h, 65%; (b) Li/NH_3, THF, −78 °C, 72 h, 66%; (c) NaH, PMBCl, TBAI, THF, 0 °C to rt, 20 h, 83%; (d) LiCl, $AcOH/H_2O$, rt, 2 h, 82%; (e) (1) 2-chloro-2-oxo-1,2,3-dioxaphospholane, DMAP, Et_3N, Tol, 0 °C, 45 min, (2) *N*,*N*-dimethyl-*N*-propargylamine, MeCN, 80 °C, 48 h, 40%; (f) (1) TFA, CH_2Cl_2, 0 °C, 30 min, (2) 4-nitrophenylstearate, Et_3N, DMAP, THF, rt, 23 h, 66%; (g) *N*-(3-azidopropyl)-dansyl amine, $CuSO_4{\cdot}5H_2O$ 10 mol %, sodium ascorbate 30 mol %, *t*-$BuOH/H_2O$ 4:1, rt, 16 h, 57%.

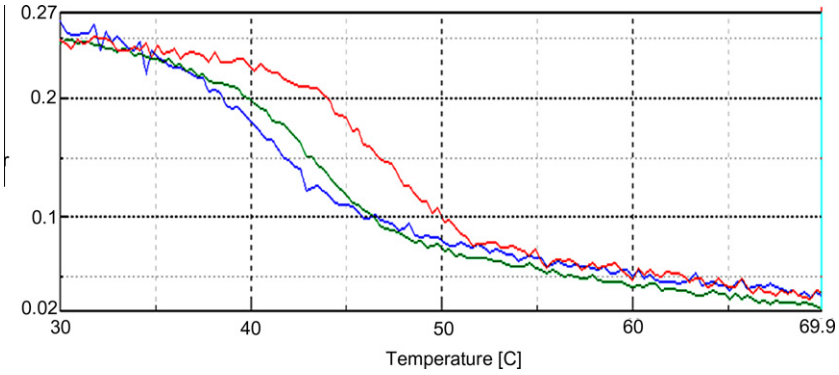

Figure 1. Temperature-dependent changes of fluorescent anisotropy (r) of SSM **1** (red, top) and its analogs **2** (green, middle)**, 3** (blue, bottom).

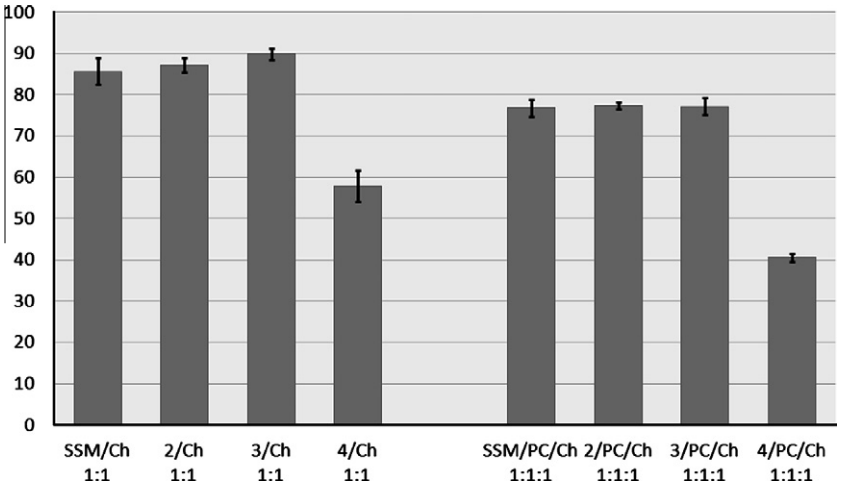

Figure 2. Detergent solubilization activities of SSM **1** and analogs **2**, **3**, and **4** as measured by percentage of retained light scattering (*y*-axis) compared to those prior to Triton-X treatment. Ch: cholesterol; PC: POPC. Error bars were derived from three experiments.

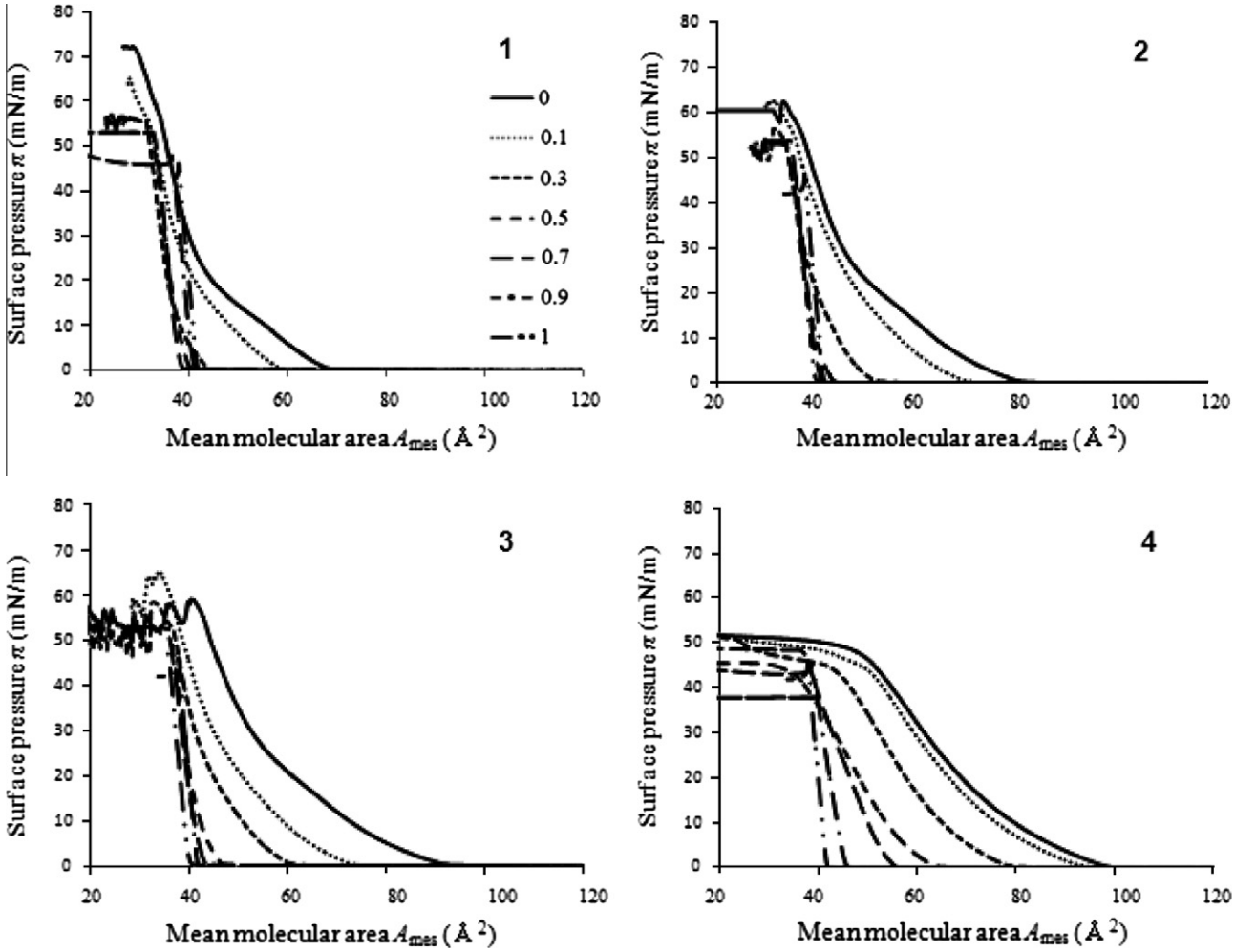

Figure 3. The surface pressure versus molecular area isotherm (π–A isotherm) of (1) **1**/Chol, (2) **2**/Chol, (3) **3**/Chol and (4) **4**/Chol mixed monolayers at 25 ± 0.1 °C. The x_{Chol} values were directly described in the figure.

corresponding to the phase transition between liquid expanded (LE) and liquid condensed (LC) phases (the solid line in Panel 1 of Fig. 3). With increasing molar fraction of Chol (x_{Chol}), the isotherm shifted toward the lower molecular area, changing its shape. The π–A isotherms of **2**/Chol, **3**/Chol and **4**/Chol mixtures showed similar x_{Chol}-dependence to the **1**/Chol mixtures (Panels **2** and **3** of Fig. 3). It should be noted that the low slope region was not observed in the π–A isotherm of pure **4** monolayer (solid line in Panel 4 of Fig. 3). Probably the monolayer stably forms the LE phase over all pressure range.

To analyze interaction between SM and Chol molecules we plotted the mean molecular areas A_{mes} as a function of x_{Chol} (Fig. 4). Here, we focused on the surface pressure at 30 mN/m because monolayers at this pressure have often been used as a model for biomembranes.[10] In the **1**/Chol mixtures, the deviations of A_{mes} from area additivity expressed by Eq. 1 were negative in all composition range, indicating that attractive interaction (condensation) occurs between **1** and Chol molecules (Panel **1** of Fig. 4). The **2**/Chol, **3**/Chol and **4**/Chol monolayers also showed smaller A_{mes} values than the area additivity in almost all composition range (Panels **2**–**4** of Fig. 4). Thus, these SM analogues attractively interact with Chol.

We next qualitatively evaluated the affinity between each SM and Chol on the basis of the excess mixing energy (ΔG_{ex}). The ΔG_{ex} value of SM/Chol mixture at given compositions was calculated by integrating the ΔA value from π = 0–30 according to Eq. 3. The mixing energy of ideal particles (ΔG_{id}) was subtracted from the Gibbs energy of mixing (ΔG_{mix}) because ΔG_{id} is independent of molecular species. In all SM/Chol mixtures, ΔG_{ex} values were found to be negative in all composition range (see the bottom panel in Fig. 4). Thus, SSM and SM analogues preferentially contact with Chol to reduce the mixing energy. In addition, **3**/Chol and **4**/Chol mixtures gave lowest ΔG_{ex} values at x_{Chol} = 0.5, which is slightly higher than that in **1**/Chol mixtures (compare squares and crosses with circles in Fig. 4). These results indicate that the **3** and **4** provide larger capacity for Chol than **1**. It is speculated that the relatively large head groups of these analogues enhance the umbrella effect, providing the large capacity for Chol (shown as the molecular areas of pure components in Fig. 4). However, the mixing energy of **4**/Chol mixtures is larger than that in the other SM/Chol mixtures, indicating that the interaction of Chol with **4** is somewhat weaker than that with the other SMs (crosses in Fig. 4). Apparently, these results are in line with the detergent solubility test, which showed the slightly higher solubility of **4**/Chol mixture than the other SM/Chol mixtures (Fig. 2).

We next examined the properties of bilayers composed of **2**/Chol and **3**/Chol in a fluid phase (50 °C) by measuring the density of membrane preparations while changing the molar fraction of Chol x_{Chol} from 0 to 0.5. Figure 5**a** shows that the specific volume (inverse density) v of the SSM/Chol mixture decreases as x_{Chol} increases and reaches a plateau at x_{Chol} = 0.25. The x_{Chol} value at which v reaches a plateau is called the critical point. Both **2**/Chol

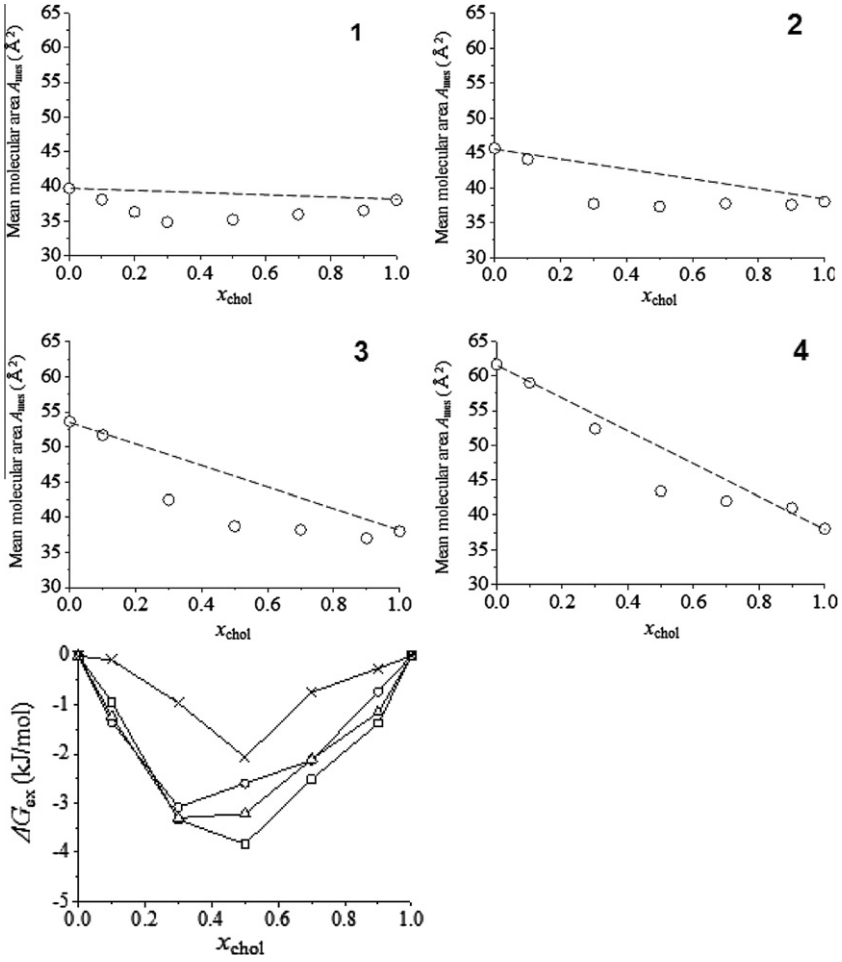

Figure 4. The mean molecular areas A_{mes} of (1) **1**/Chol, (2) **2**/Chol, (3) **3**/Chol and (4) **4**/Chol mixtures as a function of x_{Chol} at 30 mN/m. The data were obtained from Fig. 3. The dashed lines show the area additivity (A_{id}) shown by Eq. 1. Bottom panel shows the excess mixing energy ΔG_{ex} of (circles) **1**/Chol, (triangles) **2**/Chol, (squares) **3**/Chol and (crosses) **4**/Chol mixtures as a function of x_{Chol} at 30 mN/m. The data was calculated by integrating the $\Delta A(=A_{mes}-A_{id})$ over the surface pressure (π = 0–30 mN/m) according to Eq. 3.

and **3**/Chol produced the same results, although their critical point (x_{Chol} = 0.30) was slightly greater than that of SSM/Chol (Fig. 5b and c). To estimate the molecular volumes of SM in SM/Chol mixtures, the mean volumes v_{mean} of the membrane preparations were calculated and plotted as a function of x_{Chol} (Fig. 5d–f). Using specific volume v, the v_{mean} is expressed as

$$v_{mean} = (x_{Chol}) = \frac{\{x_{Chol}M_{Chol} - (1 - x_{Chol})M_{SM}\}v(x_{Chol})}{N_A}$$

where M_{Chol} and M_{SM} are molecular weights of Chol and SM, respectively, and N_A is the Avogadro's number. According to Figure 5a–c, v_{mean} versus x_{Chol} for each SM/Chol mixture fit two linear functions. The intersection between the linear function and x_{Chol} = 0 is the partial molecular volume of SM v_{SM}, indicating the effective volume of the SM/Chol mixture. A detailed description of partial molecular volume has been reported previously.[11]

In the SSM/Chol mixture, the v_{SM} value of 1226 Å^3 under the lower x_{Chol} decreased to 1205 Å^3 at x_{Chol} = 0.25 (circles in Fig. 6). This decrease in v_{SM} at the critical point is attributed to *Lo* phase formation in the SSM/Chol bilayers.[11] Both the **2**/Chol and **3**/Chol mixtures produced similar results: the v_{SM} values of **2** and **3** (1265 and 1277 Å^3, respectively) decreased to 1242 and 1245 Å^3, respectively, at x_{Chol} = 0.30 (triangles and squares in Fig. 6). Results suggest that analogs **2** and **3** interact with Chol at a stoichiometry of 2:1 (x_{Chol} = 0.30), which is approximately the same as that of SSM (x_{Chol} = 0.25). In addition, since the reductions of v_{SM} in **2**/Chol and **3**/Chol at the critical point are close to that in SSM/Chol, the condensation effect of Chol on **2** or **3** should be similar to that on SSM. The v_{SM} of SSM is less than those of **3** and **4** across the experimental range because the molecular volume of SSM is smaller than those of the analogs.

3. Discussion

This study provides the first example of chemical modification at the SM polar head and its effect on membrane properties, particularly membrane ordering effects. As depicted in Figures 1 and 2, the interactions of analogs **2** and **3** with Chol are very similar to that of SSM, demonstrating that the ammonium group can be potentially utilized for introduction of a fluorophore and other functionalities. A slight difference in the T_m values and fluorescent anisotropy curves (Fig. 1) of **1** and **2**/**3** may be due to increased volume of the head group. The loose packing of pure lipid bilayers formed by **2** or **3** may weaken intermolecular attraction, leading to T_m values lower than that of SSM.

Hydrophobic substituents such as a dansyl group in **4** may prevent formation of stable ordered domains as shown by the detergent solubilizing assays and π–*A* experiments (Figs. 2–4). However, **4** interacts with Chol to a certain extent, and partly forms detergent-resistant domains, implying that, even with a fluores-

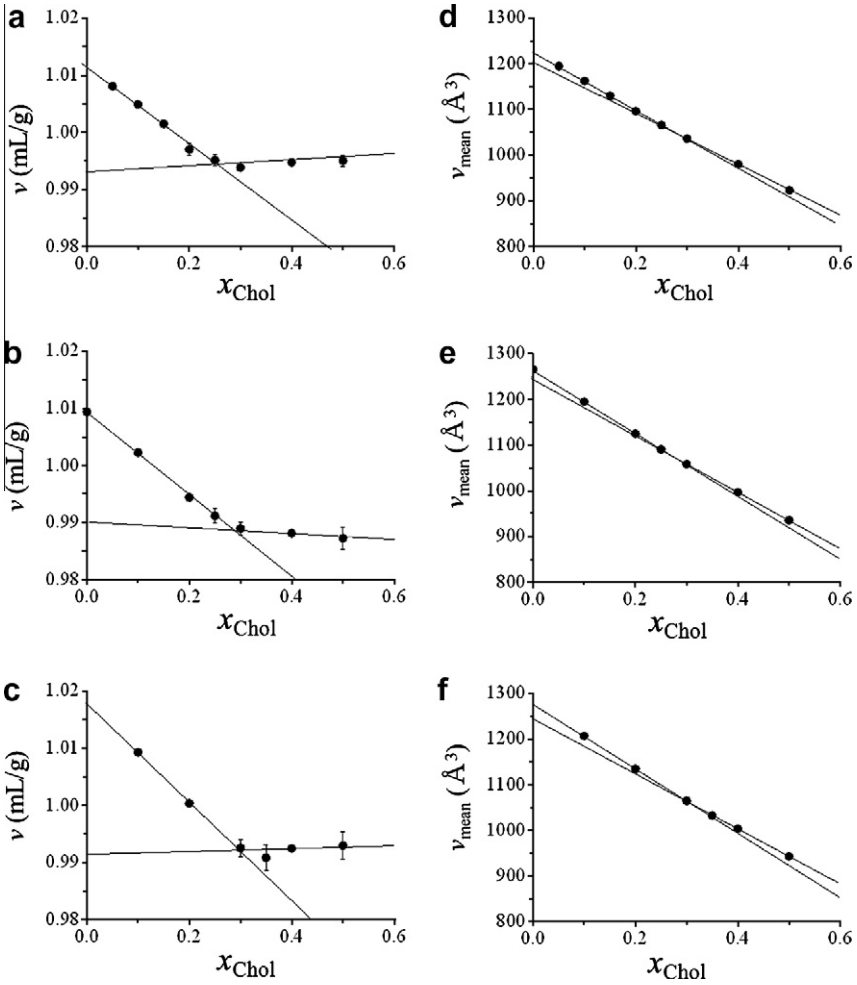

Figure 5. Chol concentration dependence of specific volume v of: (a) SSM/Chol, (b) **2**/Chol, and (c) **3**/Chol mixtures at 50 °C (fluid phase). The v versus x_{Chol} plot for each SM/Chol mixture fits two linear functions (solid lines), which intersect at critical point x_{Chol} = 0.25 for the SSM/Chol mixture and x_{Chol} = 0.30 for the **2**/Chol and the **3**/Chol mixtures. Chol concentration dependence of the mean molecular volume v_{mean} of: (d) SSM/Chol, (e) **2**/Chol, and (f) **3**/Chol mixtures at 50 °C. The v_{mean} value was estimated from v. According to the v *versus* x_{Chol} plot, the v_{mean} fit two linear functions (solid lines) as a function of x_{Chol}.

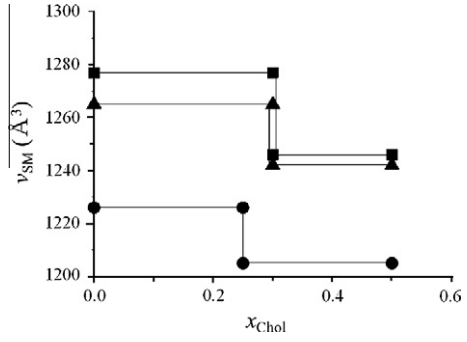

Figure 6. Partial molecular volumes of SMs v_{SM} in: SSM/Chol (circles), **2**/Chol (triangles), and **3**/Chol (squares) at 50 °C. The v_{SM} value was obtained from the intersection between linear functions and x_{Chol} = 0.

cent group, N-substituted SM retained the ability to form microdomain with Chol. Dansyl group are of interest because of its usefulness in FRET experiments for examining interactions with a tryptophan residue, which is thought to play an essential role in SM membrane recognition. In addition, the aromatic residue exerts an anchoring effect, which stabilizes membrane proteins so they can assume the correct position in the bilayer membranes. Thus, a dansyl group or other fluorophore having an excitation maximum ca. 340 nm is a potential target for developing fluorescent lipid probes. Results of this study indicate that **4** may promote an ordered phase when added as a minor constituent, such as in the case of a fluorescent-labeled molecular probe. We thus attempted to observe the distribution of **4** in membrane containing microdomains using a confocal microscope. Due to the rapid bleaching of fluorescence of the dansyl group coupled with its shorter excitation wavelength, however, it has not been successful so far to observe the localization of **4** on bilayer membranes. More hydrophilic fluorophores with longer excitation wave length that could be tagged to the head group of SM or other lipids via an ammonium group would be a potential raft-specific/selective probe that could distinguish lipid rafts[12] with different lipid constituents on cellular membranes. Research on the preparation of these probes is now underway.

As reported by Yamakoshi et al.[13] an alkyne group can be observed selectively in living cells by Raman microscopy. Thus, the triple-bond-bearing analog **2** may be utilized as a bioorthogonal 'Raman tag' for bioimaging. As often seen in membrane biology and biophysics, a large fluorescent tag inherently disrupts the physiological functions of biomolecules, particularly smaller molecules such as lipids. Thus, small alkyne groups, including an ethynyl (only 25 Da), may serve as a versatile labeling functionality.

4. Experimental

4.1. Synthesis of SM analogues 2, 3, and 4

See Supplementary data including NMR chemical shift data.

4.2. Materials

Palmitoryl oleoyl phosphatidylcholine (POPC) was purchased from Avanti Polar Lipids (Alabaster, AL). Cholesterol and Triton X-100 were purchased from Nakarai Tesque (Kyoto, Japan). Diphenylhexatriene (DPH) was purchased from Aldrich (St. Louis, MO). Bovine brain sphingomyelin (SM) was purchased from Avanti Polar Lipids (Alabaster, AL), and 18-0 SM was purified from the brain sphingomyelin (SM) using HPLC.

4.3. Differential scanning calorimetry (DSC)

The main transition temperatures of pure SSM and analog **2** and **3** bilayers were examined by DSC. Samples were prepared using a conventional method. Briefly, the appropriate amount of SSM, **2**, or **3** powder was dispersed in 10 mM HEPES buffer (pH 7.6) and incubated at 55 °C for 10 min with intermittent vortexing. Final lipid concentration of the sample was 13 wt %. Then, 10–15 μL of the sample (1.3–2.0 mg of lipids total) were enclosed in the aluminum pane 0219-0062 (Perkin–Elmer, California) and put into the DSC instrument (Diamond, Perkin–Elmer, California) immediately before measurements were obtained. The DCS temperature was calibrated using representative phospholipid bilayers with known transition temperatures: DMPC (24.5 °C), DPPC (41.5 °C), and DSPG (53.5 °C). A scanning rate of 5.0 °C/min was used for all DSC measurements.

4.4. Percent solubilization experiments

Sample preparation for solubility experiments involved drying a MeOH-$CHCl_3$ solution of 500 nmol of total lipid (SM and sterol) under a stream of argon, followed by redissolution in chloroform, and then drying again under a stream of argon. After the lipids were dried further under high vacuum for at least 12 h, they were hydrated (swelled) by adding 0.95 mL PBS buffer (pH 7). To uniformly disperse the lipids and form homogeneous multilamellar lipid vesicles, each sample was vigorously vortexed at a temperature of 65 °C, well above the phase transition temperature of SM, and then cooled to room temperature. For measuring solubilization by the loss of light scattering, the optical density of these samples was measured at 400 nm on a Shimadzu UV-2500 spectrophotometer. Then, 50 μL of 10% (w/v) Triton X-100/PBS was added. After mixing and incubating at 23 °C for 2 h, the optical density was remeasured. The ratio of optical density (%OD) after Triton X-100 incubation (not corrected for dilution with Triton X-100 solution) to that before the addition of Triton X-100, was then calculated.

4.5. Fluorescent polarization measurements

Multilamellar vesicles of lipids containing 2 mol % DPH were prepared by drying a MeOH–$CHCl_3$ solution containing 160 nmol of total lipids (phospholipids and sterol) and 3.2 nmol of DPH under a stream of argon. The residue was redissolved in $CHCl_3$, and dried again under a stream of argon. After the lipids were dried further under high vacuum for at least 12 h, they were hydrated (swelled) by adding 3 mL of PBS buffer (pH 7.0). To uniformly disperse the lipids and form homogeneous multilamellar lipid vesicles, each sample was vigorously vortexed at a temperature of 65 °C, well above the phase transition temperature of SM, and then cooled to room temperature. The samples were freeze-thawed three times by cycling the samples between liquid nitrogen and a water bath maintained at 65 °C. Fluorescence polarization measurements were performed with a JASCO FP-6600 spectrofluorometer equipped with a JASCO ADP-303 polarization accessory. Quartz cuvettes with a path length of 1 cm were used. The excitation wavelength was set at 358 nm and emissions were monitored at 430 nm. Excitation and emission slits with bandpasses of 1 and 10 nm, respectively, were used for all measurements. The smallest possible excitation slit was used to minimize any photoisomerization of DPH during irradiation. Measurement temperature was raised from 30 °C to 70 °C at 2 °C/min, and fluorescence was measured with a 2 s response. Polarization values were calculated using Spectra Manager software attached to the spectrofluorometer.

4.6. π–A isotherm measurements of monlayers

Monolayers of SM/Chol mixtures were prepared on a computer-controlled Langmuir-type film balance (USI System, Fukuoka, Japan) calibrated by stearic acid. The subphase was distilled and freshly deionized water from Milli-Q system (Millipore Corp.). The apparatus was covered with a vinyl sheet, which prohibited dust from depositing on the water surface. Thirty micro-liters of lipid solution (1 mg/mL) were spread onto the aqueous subphase (100×290 mm^2) with a glass micropipette (Drummond Scientific Company, Pennsylvania, USA). The monolayers were compressed at a rate of 10–20 mm^2/s after the initial delay period of 10 min for evaporation of organic solvents. The subphase temperature was controlled to be 25.0 ± 0.1 °C. We repeated the measurements several times under the same conditions to obtain reliable results. These measurements gave the molecular areas at the corresponding pressure within the error of ±0.01 nm^2.

We evaluated the intermolecular interaction between SM and Chol at the surface pressure of 30 mN/m on the basis of the deviations of experimentally obtained mean molecular areas (A_{mes}) from those of ideal mixtures (A_{id});

$$A_{id} = A_{SM}x_{SM} + A_{Chol}x_{Chol}, \quad (1)$$

where A_{SM} and A_{Chol} are the molecular areas of pure SM and Chol, and x_{SM} and x_{Chol} are molar fractions of SM and Chol, respectively. The value of A_{id} corresponds to the mean molecular area in the mixture constituted of non-interactive or completely immiscible molecules. The negative deviation of A_{mes} from A_{id} ($\Delta A = A_{mes} - A_{id} < 0$) indicates attractive lateral intermolecular interactions between two molecules.

We calculated the excess Gibbs energy of mixing, ΔG_{ex}, to definitively evaluate the affinity of the SM analogue and Chol.

$$\Delta G_{ex} = \Delta G_{mix} - \Delta G_{id} = \Delta G_{mix} - RT(x_{SM}\ln x_{SM} + x_{Chol}\ln x_{Chol}), \quad (2)$$

where R is the gas constant and T is absolute temperature. The mixing energy of ideal particles (ΔG_{id}) is subtracted from the Gibbs energy of mixing (ΔG_{mix}) because ΔG_{id} is independent of molecular species. According to Goodrich[14] ΔG_{ex} was calculated as an integral of the deviation, ΔA, over the surface pressure π;

$$\Delta G_{ex} = \int_0^{\pi} (\Delta A)d\pi = \int_0^{\pi} (A_{mes} - A_{SM}x_{SM} - A_{Chol}x_{Chol})d\pi \quad (3)$$

4.7. Density measurements

According to Nagle and others, the neutral floatation method allows the specific volume (inverse density) of a bilayer sample to be estimated using H_2O/D_2O mixtures as a solvent.[15] Theoretically, the specific volumes of H_2O and D_2O can be defined as v_{H2O} and v_{D2O}, respectively. Thus, the specific volume of solvent v_{sol} is defined as:

$$v_{sol} = \varphi v_{D2O} + (1 - \varphi) v_{H2O},$$

where φ is the mass fraction of D_2O. If the specific volume of the lipid vesicle v is larger than v_{sol}, the vesicle floats in the H_2O/D_2O solvent. If v is smaller than v_{sol}, the vesicle sinks in the solvent. The floating/sinking process can be facilitated by centrifugation. When the sample is obtained in the supernatant with the specific volume of v_{sol}^{sup} and the precipitate comes out of solution involving the solvent with v_{sol}^{pre}, the specific volume of sample v can be determined using the following equation:

$$v = \frac{v_{sol}^{sup} + v_{sol}^{pre}}{2} \pm \frac{v_{sol}^{sup} - v_{sol}^{pre}}{2}$$

Experimentally, a solution containing the appropriate amounts of SM and Chol co-dissolved into MeOH/$CHCl_3$ (1:4 v/v) (Wako Pure Chemical Industries, Ltd., Osaka, Japan) was dried under nitrogen flow and stored under high vacuum for more than 24 h to remove all organic solvent. The dried sample was dispersed into H_2O/D_2O (Wako Pure Chemical Industries, Ltd, Osaka, Japan) and incubated at 50 °C for several minutes with intermittent vortexing. Final lipid concentration was ~5 mM.

The incubated sample was rapidly transferred into a centrifuge (Kubota 1910, Kubota Co., Ltd, Tokyo, Japan) and centrifuged (20,000×*g*) for 5–20 min at 55 °C, a temperature at which all samples formed a fluid phase. Sample temperature (K) was measured directly with a thermometer (AD-5602A Sansyo Industries, Ltd, Tokyo, Japan) immediately after centrifugation. When the sample was reused, it was heated and cooled several times around the main transition temperature after addition of H_2O or D_2O. Because voids or packing defects appear in the lipid membranes near the transition temperature, the heating/cooling cycles achieve homogeneous v_{sol} between the outer and the inner portions of a lipid vesicle.

Acknowledgments

We are grateful to Professor J. Peter Slotte, Åbo Akademi University, Professor Mikiko Sodeoka, Dr. Jun Ando, Dr. Hiroyuki Yamakoshi, Riken, Professor Tohru Oishi, Kyushu University, and Dr. Fuminori Satou, this ERATO project for discussions. This work was supported in part by Grant-In-Aids for Scientific Research (S) (No. 18101010), and (B) (No. 20310132) from MEXT, Japan and by a SUNBOR grant from the Suntory Institute for Bioorganic Research. A research fellowship to S.A.G. from the Japan Society for the Promotion of Science (JSPS) is greatly appreciated.

Supplementary data

Supplementary data associated with this article can be found, in the online version, at http://dx.doi.org/10.1016/j.bmc.2012.05.015.

References and notes

1. Simons, K.; Ikonen, E. *Nature* **1997**, *387*, 569.
2. Some recent reviews; (a) Bagatolli, L. A.; Ipsen, J. H.; Simonsen, A. C.; Mouritsen, O. G. *Prog. Lipid Res.* **2010**, *49*, 378; (b) Kusumi, A.; Shirai, Y. M.; Koyama-Honda, I.; Suzuki, K. G. N.; Fujiwara, T. K. *FEBS Lett.* **1814**, *2010*, 584; (c) Levental, I.; Grzybek, M.; Simons, K. *Biochemistry* **2010**, *49*, 6305; (d) Elson, E. L.; Fried, E.; Dolbow, J. E.; Genin, G. M. *Annu. Rev. Biophys.* **2010**, *39*, 207.
3. (a) Eggeling, C.; Ringemann, C.; Medda, R.; Schwarzmann, G.; Sandhoff, K.; Polyakova, S.; Belov, V. N.; Hein, B.; von Middendorff, C.; Schönle, A.; Hell, S. W. *Nature* **2009**, *457*, 1159; (b) Rosseto, R.; Tcacenco, C. M.; Ranganathan, R.; Hajdu, J. *Tetrahedron Lett.* **2008**, *49*, 3500.
4. Sandbhor, M. S.; Key, J. A.; Strelkov, I. S.; Cairo, C. W. *J. Org. Chem.* **2009**, *74*, 8669.
5. (a) Nyholm, T.; Nylund, M.; Soderholm, A.; Slotte, J. P. *Biophys. J.* **2003**, *84*, 987; (b) Zhao, H.; Jutila, A.; Nurminen, T.; Wickstrom, S. A.; Keski-Oja, J.; Kinnunen, P. K. J. *Biochemistry* **2005**, *44*, 2857; (c) Ran, Y.; Fanucci, G. E. *Anal. Biochem.* **2008**, *382*, 132; (d) Smirnova, I. N.; Kasho, V. N.; Kaback, H. R. *Biochemistry* **2006**, *45*, 15279; (e) Haldar, S.; Raghuraman, H.; Chattopadhyay, A. *J. Phys. Chem. B* **2008**, *112*, 14075; (f) Ramirez, D. M. C.; Ogilvie, W. W.; Johnston, L. J. *Biochim. Biophys. Acta, Biomembr.* **2010**, *1798*, 558; (g) Cai, Y.; Ling, C. C.; Bundle, D. R. *Org. Biomol. Chem.* **2006**, *4*, 1140.
6. Blot, V.; Jacquemard, U.; Reissig, H.-U.; Kleser, B. *Synthesis* **2009**, 759.
7. (a) Radunz, H. E.; Devant, R. M.; Eiermann, V. *Liebigs Ann. Chem.* **1988**, 1103; (b) Herold, P. *Helv. Chim. Acta* **1988**, *71*, 354; (c) Garner, P.; Park, J. M.; Malecki, E. *J. Org. Chem.* **1988**, *53*, 4395; (d) Nimkar, S.; Menaldino, D.; Merrill, A. H.; Liotta, D. *Tetrahedron Lett.* **1988**, *29*, 3037; (e) Soai, K.; Takahashi, K. *J. Chem. Soc., Perkin Trans. 1* **1994**, 1257; (f) Azuma, H.; Tamagaki, S.; Ogino, K. *J. Org. Chem.* **2000**, *65*, 3538; (g) Murakami, T.; Furusawa, K. *Tetrahedron* **2002**, *58*, 9257; Chun, J.; Li, G.; Byun, H.-S.; Bittman, R. *Tetrahedron Lett.* **2002**, *43*, 375; (i) Suzuki, H.; Mori, M.; Shibakami, M. *Synlett* **2003**, 2163; (j) Sawatzki, P.; Kolter, T. *Eur. J. Org. Chem.* **2004**, 3693; (k) Murakami, T.; Furusawa, K.; Tamai, T.; Yoshikai, K.; Nishikawa, M. *Bioorg. Chem. Med. Lett.* **2005**, *15*, 1115; (l) Okamoto, N.; Kanie, O.; Huang, Y.-Y.; Fujii, R.; Watanabe, H.; Shimamura, M. *Chem. Biol.* **2005**, *12*, 677; (m) Reference 6c.; (n) Ohshita, K.; Ishiyama, H.; Takahashi, Y.; Ito, J.; Mikami, Y.; Kobayashi, J. *Bioorg. Med. Chem.* **2007**, *15*, 4910.
8. (a) Kim, H.-Y.; Sohn, J.; Wijewickrama, G. T.; Edirisinghe, P.; Gherezghiher, T.; Hemachandra, M.; Lu, P.-Y.; Chandrasena, R. E.; Molloy, M. E.; Tonetti, D. A.; Thatcher, G. R. J. *Bioorg. Med. Chem.* **2010**, *18*, 809; (b) Landi, F.; Johansson, C. M.; Campopiano, D. J.; Hulme, A. N. *Org. Biomol. Chem.* **2009**, *8*, 56; (c) Zhang, X.; Cao, B.; Yu, S.; Zhang, X. *Angew. Chem., Int. Ed.* **2010**, *49*, 4047.
9. Schnitzer, E.; Kozlov, M. M.; Lichtenberg, D. *Chem. Phys. Lipids* **2005**, *135*, 69.
10. (a) Demel, R. A.; Geurts van Kessel, W. S. M.; Zwaal, R. F. A.; Roelofsen, B.; Van Deenen, L. L. M. *Biochim. Biophys. Acta* **1975**, *406*, 97; (b) Nagle, J. F. *J. Membr. Biol.* **1976**, *148*, 997; (c) Blume, A. *Biochim. Biophys. Acta* **1979**, *577*, 32; (d) Feng, S. S. *Langmuir* **1999**, *15*, 998; (e) Zhai, X.; Li, X. M.; Momsen, M. M.; Brockmann, H. L.; Brown, R. E. *Biophys. J.* **2006**, *91*, 2490.
11. Greenwood, A. I.; Tristram-Nagle, S.; Nagle, J. F. *Chem. Phys. Lipids* **2006**, *143*, 1.
12. As to raft heterogeneity, for examples, (a) GomezMouton, C.; Abad, J. L.; Mira, E.; Lacalle, R. A.; Gallardo, E.; Jimenez-Baranda, S.; Illa, I.; Bernad, A.; Manes, S.; Martinez-A, C. *Proc. Natl. Acad. Sci. U.S.A.* **2001**, *98*, 9642; (b) Bagnat, M.; Simons, K. *Proc. Natl. Acad. Sci. U.S.A.* **2002**, *99*, 14183; (c) Pike, L. J. *Biochem. J.* **2004**, *378*, 281; (d) Kiyokawa, E.; Baba, T. K.; Otsuka, N.; Makino, A.; Ohno, S.; Kobayashi, T. *J. Biol. Chem.* **2005**, *280*, 24072; (e) Lingwood, D.; Kaiser, H.-J.; Levental, I.; Simons, K. *Biochem. Soc. Trans.* **2009**, *37*, 955.
13. Yamakoshi, H.; Dodo, K.; Okada, M.; Ando, J.; Palonpon, A.; Fujita, K.; Kawata, S.; Sodeoka, M. *J. Am. Chem. Soc.* **2010**, *133*, 6102.
14. Goodrich, F. C. Molecular interaction in mixed monolayer In *Second International Congress on Surface Activity*; Schulman, J. H., Ed.; Butterworth & Co.: London, 1957; Vol. I, p 85.
15. (a) Nagle, J. F.; Wilkinson, D. A. *Biophys. J.* **1978**, *23*, 159; (b) Wiener, M. C.; Tristram-Nagle, S.; Wilkinson, D. A.; Campbell, L. E.; Nagle, J. F. *Biochim. Biophys. Acta* **1998**, *938*, 135; (c) Koenig, B. W.; Gawrisch, K. *Biochim. Biophys. Acta* **2005**, *1715*, 65.